frontiers in Materials

ORIGINAL RESEARCH
published: 21 March 2022
doi: 10.3389/fmats.2022.848123

# Hydrogen Permeation Behavior of Carbon Steel During Corrosion in Highly Pressed Saturated Bentonite

*Qichao Zhang[1,2], Yishan Jiang[2], Xin Zhao[2], Penglei Song[2], Tingting Kuang[1], Juna Chen[2], Zhongtao Sun[2], Yaopeng Zhang[2], Xiayu Ai[2], Dongzhu Lu[1]* and Yanliang Huang[1]**

[1]CAS Key Laboratory of Marine Environment of Corrosion and Bio-fouling, Institute of Oceanology, Chinese Academy of Sciences, Qingdao, China, [2]Navy Submarine Academy, Qingdao, China

Deep geological disposal is the most reliable method for high-level nuclear waste, of which metal container as the first barrier for deep geological disposal of high-level nuclear waste is particularly important. Carbon steel is used as a container material because of the low possibility of local corrosion in bentonite. However, after the storage is closed, the decrease of oxygen content will create a near-field environment where the hydrogen embrittlement (HE) in the corrosion process of the container could happen. To evaluate the safety of containers in deep geological disposal of Beshai, the preselected area in China, hydrogen permeation efficiency and HE were estimated in highly pressed saturated bentonite by electrochemical and extrapolation analyses. It is concluded that hydrogen permeation efficiency increases with the disposal year, which proves that the hydrogen evolution reaction dominates the cathode process in the corrosion during long-term disposal. However, slow strain rate tensile shows that Q235 steel has a low HE sensitivity.

**Keywords: hydrogen embrittlement, metal corrosion, hydrogen permeation, bentonite, nuclear waste**

OPEN ACCESS

***Edited by:***
*Qixin Zhou,*
*University of Akron, United States*

***Reviewed by:***
*Long Hao,*
*Corrosion and Protection Center of Materials, Institute of Metal Research Chinese Academy of Sciences, Shenyang, China*
*Ang Liu,*
*Qingdao University of Technology, China*

****Correspondence:***
*Dongzhu Lu*
*421241006@qq.com*
*Yanliang Huang*
*263342066@qq.com*

***Specialty section:***
*This article was submitted to Environmental Degradation of Materials, a section of the journal Frontiers in Materials*

***Received:*** *04 January 2022*
***Accepted:*** *21 January 2022*
***Published:*** *21 March 2022*

***Citation:***
*Zhang Q, Jiang Y, Zhao X, Song P, Kuang T, Chen J, Sun Z, Zhang Y, Ai X, Lu D and Huang Y (2022) Hydrogen Permeation Behavior of Carbon Steel During Corrosion in Highly Pressed Saturated Bentonite. Front. Mater. 9:848123. doi: 10.3389/fmats.2022.848123*

## INTRODUCTION

As low-carbon energy, nuclear power plays an important role in new energy and is an important basis for realizing the sustainable development of energy in various countries. High-level nuclear waste (HLNW) produced during the use of nuclear energy has the characteristics of strong radioactivity of calorific value, high toxicity, and extremely long decay time (Zhang et al., 2020). According to the nuclear power development plan in China, it is expected that there will be produced 3,200 tons of nuclear waste every year in 2030. Therefore, the safe disposal of nuclear waste is an unavoidable and urgent problem in the development of nuclear energy.

The disposal of nuclear waste is a difficult problem globally (Shoesmith, 2000; Hu and Cheng, 2015). At present, deep geological disposal is the most reliable technology for the disposal of HLNW (Ewing, 2015); that is, nuclear waste solidified in glass is stored in the metal container, surrounded by clay and other buffer materials, then placed in the special disposal repository situated between 500 and 1,000 m underground.

How to deal with nuclear waste efficiently has become a global problem. Various nuclear waste disposal programs have been proposed in the world: space disposal, deep-sea disposal, deep geological disposal, etc. (Arup, 1985; Milnes, 1985; Bradley, 1997). At present, deep geological disposal is generally accepted as the most realistic treatment (Duquette et al., 2009; Guo et al., 2020); that is, nuclear waste will be buried in a disposal repository approximately 500–1,000 m underground, making it completely isolated from the human living environment. Now, China

has selected the Beishan area of Gansu Province as the preselected area of high-level nuclear disposal. The repository contains a "multi-barrier protection system" with engineering barriers including vitrified waste bodies, metal containers, buffer backfill materials, and natural barriers including surrounding rocks, its surrounding geological constructions. Among them, the metal container as the first engineering barrier is particularly important, and its integrity is a necessary factor to ensure that the nuclear waste does not leak. Once the corrosion of the metal container happens during the long disposal process, nuclear waste will migrate with groundwater into the biosphere. It is necessary to study various factors that affect the corrosion behavior of containers in deep geological environments to evaluate the container's safety and reliability.

Container corrosion is related to its surrounding environment. It mainly includes oxygen content (after the repository closed and some oxygen trapped), temperature (nuclear waste decay heat release), and radiation (strong radioactivity of nuclear waste), which are the factors affecting the container corrosion in the deep geological environment. However, the near-field environment of the container will change with the disposal year. For example, the temperature will experience a rise to a drop (up to 360 K), the oxygen content will drop to an anaerobic condition, and the γ radiation intensity will also decrease. Carbon steel is used as a candidate material for the container in countries such as Japan, South Korea, and Canada because of its simple manufacturing process and low cost (King and Padovani, 2011). Liu et al. (2019a, b) studied the corrosion behavior of X65 low-carbon steel during the low-oxygen transition and the anaerobic stage of geological disposal. The results show that the corrosion type is mainly uniform corrosion. The corrosion rate decreases significantly with oxygen reduction, and the corrosion process is controlled by diffusion. The authors' group (Zhang et al., 2019) studied the corrosion behavior of Q235 steel in the highly pressed bentonite environment. It is shown that the maximum corrosion rate appeared in the range of 343–363 K and then decreased when the temperature decreased. Stoulil et al. (2013) studied the effect of temperature on the corrosion rate of low-carbon steel in bentonite environments, and the experiments were carried out at 313 and 363 K. The results show that the higher the temperature, the denser the corrosion product layer, the corrosion rate is slightly slower than that at 313 K, and the color of the corrosion product formed at different temperatures is different. Liu et al. (2018) studied the effect of γ irradiation on the corrosion behavior of X65 low-carbon steel in deep geological groundwater environments. It was found that irradiation increases the empty potential strength of the carbon steel and reduces the open circuit potential, thus accelerating the corrosion rate. Smart et al. (2008) separately studied the effects of different irradiation intensities on the anaerobic corrosion of carbon steel and found that irradiation can increase the corrosion rate. At the higher dose rate, the radiation enhances the corrosion rate most, and some unknown high oxidative corrosion products form.

However, after the repository construction is finished, the oxygen content around the container decreases rapidly and even returns to an anaerobic environment, and hydrogen evolution corrosion may play an important role. The research shows that even under the condition of aerobic corrosion, the reduction of hydrogen ions will also happen, and hydrogen will permeate into carbon steel (Huang and Zhu, 2005; Tsuru et al., 2005). Therefore, hydrogen evolution corrosion will accompany the whole corrosion process of the container. The results reflect that although low-carbon steel shows low sensitivity to stress corrosion and hydrogen embrittlement (HE), its plasticity decreases in slow strain rate tensile (SSRT) under hydrogen charging. The container has circumferential tensile stress under decay thermo-mechanical coupling, up to 57% of the tensile strength (Zhang et al., 2013). During the long disposal process, the container may also be damaged by strong crustal movement such as an earthquake. Therefore, due to the long-term permeation of hydrogen into carbon steel, there may be a risk of HE, which needs to be studied. In this paper, the hydrogen permeation efficiency (HPE) and HE sensitivity of Q235 steel in highly pressed bentonite were studied by accelerated electrochemical test and SSRT. The possibility of HE for Q235 steel as the nuclear waste container on a large time scale was comprehensively analyzed and evaluated.

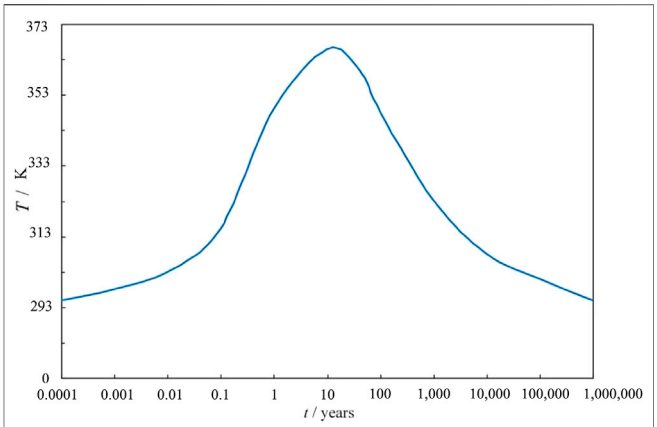


**FIGURE 1 |** Temperature evolution with time near HLNW container for China.

# EXPERIMENTAL

## Materials

For the specimens used in the corrosion electrochemical test, the carbon steel materials were cut to dimensions of ϕ10 × 10-mm columnar specimens, which were cleaned with absolute ethanol and dried in the cold air. The copper conductor was attached to one end of the specimen and sealed in a polytetrafluoroethylene tube with epoxy resin, and the other end is the working surface with an area of 0.785cm$^2$. For the specimens used in the hydrogen permeation electrochemical test, hollow barrel specimens with dimensions of ϕ40 mm × 100 mm were obtained. For the SSRT test, circular carbon steel specimens with a cross-sectional radius of 2 mm and a gauge length of 25mm were used.

**TABLE 1 |** Predicted temperature corresponding to disposal time.

| *T*/K | 363 | 348 | 340 | 323 | 308 | 301 |
|---|---|---|---|---|---|---|
| *t*/years | 10 | 100 | 300 | 1,000 | 10,000 | 100,000 |

## Corrosion Environment Simulation

As we know that the corrosion behavior of metal materials is closely related to their surrounding environment, it is necessary to determine the near-field environment of a nuclear waste container. Nuclear waste containers need to be buried in deep geological disposal for tens of thousands or even hundreds of thousands of years, and the near-field environment will change over time. At present, most studies focus on models to simulate them. The environmental conditions mainly include the following aspects: 1) Temperature. The change of temperature is mainly due to the heat generated by the decay of radionuclides, which is mainly transmitted from the nuclear waste through radiation, convection, and conduction (Seetharam et al., 2006). The evolution law is shown in **Figure 1**. For the deep geological disposal of China's HLNW, the lowest temperature is approximately 295 K, and the temperature reaches the maximum of 363 K after 10 years. This paper mainly evaluates the life of the container on a large time scale, so it focuses on the situation after 10 years. The experiment will use a gradient cooling method by a thermostat or a water bath to simulate the real environmental temperature drop after 10 years. The corresponding age to a specific temperature is shown in **Table 1**. (2) groundwater composition. Zheng et al. (2016) summarized composition of groundwater in Beishan, which is mainly alkaline, including cations such as $Na^+$ and $K^+$, while anions including $HCO3^-$, $Cl^-$, and so on. Components of artificial groundwater simulation solution used in experiment are shown in **Table 2**. (3) Buffer backfill materials. There are two kinds of materials to choose from. Sweden, Finland, and Canada (Rasilainen, 2004; Rosborg and Werme, 2008) used bentonite as a buffer backfill material, whereas Belgium used concrete (Yang et al., 2008). This paper mainly focuses on corrosion behavior of container in bentonite as a buffer backfill material. Components are shown in **Table 3**.

According to **Figure 2**, the groundwater in the buffer backfill material is saturated in approximately 10 years. Therefore, the life prediction of the container on a large time scale is more concerned about the situation after the bentonite reaches saturation.

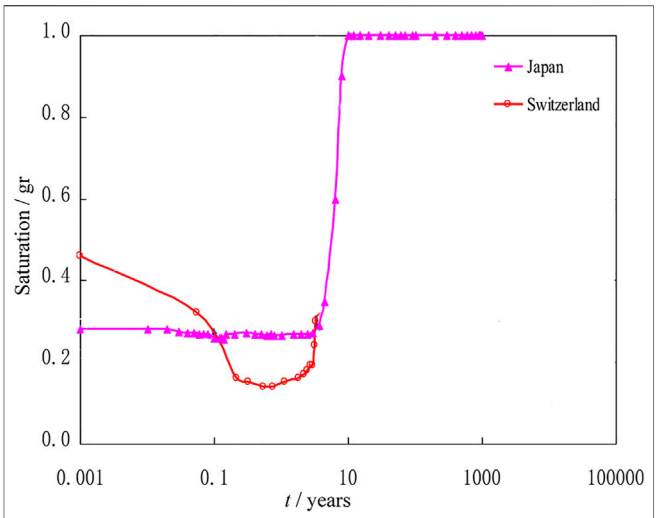


**FIGURE 2 |** Model of buffer material saturation for HLNW container in short- and long-term.

## Experimental Setups and Procedures

As shown in **Figure 3**, it is the device including the hydrogen charging and measurement system for researching the HPE of carbon steel in saturated highly pressed bentonite. The barreled specimen was filled with highly pressed saturated Gaomiaozi-Na-bentonite with simulated groundwater solution as a wetting solution. The measurement was carried out by Model PS-8 Multichannel Potentiostat/Galvanostat. For the hydrogen charging system, a three-electrode system was adopted, the working electrode was the barreled carbon steel specimen, the internal reference was a solid Ag/AgCl electrode, and the counter electrode was the stainless steel shaft (also used as the pressing bentonite device). For the hydrogen measurement system, the three-electrode system was also used, the barreled specimen was still used as the working electrode, the external reference electrode was the HgO/Hg electrode, and the stainless steel barrel wrapped with the carbon steel specimen was the counter electrode. The solution between the specimen and the stainless steel barrel was filled with 0.2 mol $L^-$ NaOH solution. Constant current densities of 0.01–100 A $m^{-2}$ were used for the hydrogen charging system, and a constant potential of 0 V *vs.* (HgO/Hg) was used for the hydrogen measurement system. A thermostated water bath was used to control the temperatures from 298 to 373 K.

As shown in **Figure 4**, the total amount of hydrogen evolution was calculated by subtracting the background current and then integrating the amount of the area under the curve. According to the volume V of the specimen and the formula (1), combined with Faraday's law, the hydrogen concentration in the specimen could finally be calculated.

$$C_H = Q_H/V\,(\mathrm{mg\,m^{-3}}) \quad (1)$$

**TABLE 2 |** Simulated chemical components of groundwater in Beishan area (mg/L).

| Component | $NaNO_3$ | KCl | $NaHCO_3$ | $MgSO_4{\cdot}7H_2O$ | $CaCl_2$ | NaCl | $Na_2SO_4$ |
|---|---|---|---|---|---|---|---|
| Content | 37.153 | 38.205 | 138.418 | 571.585 | 579.193 | 1,487.465 | 1,577.697 |

**TABLE 3 |** Chemical compositions of Gaomiaozi-Na-bentonite (mass fraction/%).

| Component | $Al_2O_3$ | $SiO_2$ | $P_2O_5$ | CaO | $K_2O$ | $TiO_2$ | FeO | $TFe_2O_3$ | MgO | $Na_2O$ | MnO | Loss on ignition |
|---|---|---|---|---|---|---|---|---|---|---|---|---|
| Mass fraction | 14.24 | 68.40 | 0.05 | 0.99 | 0.68 | 0.14 | 0.26 | 2.53 | 3.31 | 1.62 | 0.036 | 7.67 |

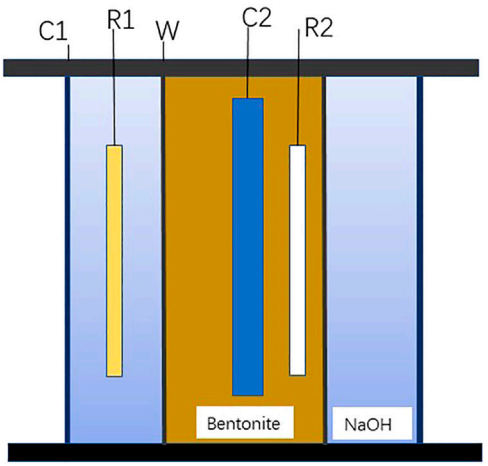


**FIGURE 3 |** Double electrolytic cell device for hydrogen permeation test of Q235 steel in saturated compacted bentonite.

SSRT mainly judges the HE risk of candidate material for a container. Because hydrogen diffuses extremely quickly in steel, a group control test was carried out: 1) The specimen was not treated in any way and exposed to the air for the tensile test; 2) the specimen was not treated in any way and immersed in 0.2 mol $L^{-1}$ NaOH solution for the tensile test; 3) the specimen was charging in 0.2 mol $L^{-1}$ NaOH solution with a current density of 1 mA $cm^{-2}$ for 15 h and 7 days and then exposed to the air for the tensile test; 4) the tensile test was carried out while the specimen charging in 0.2 mol $L^{-1}$ NaOH solution with current densities of 0.01 and 1 mA $cm^{-2}$. The morphology of the fracture surface was observed by scanning electron microscope. The experiments discussed earlier were performed at room temperature.

# RESULTS AND DISCUSSION

## Effect of γ Radiation on Corrosion

The effect of radiation on hydrogen permeation mainly depends on the effect on the steel corrosion behavior. Thus, the effect of γ radiation on steel corrosion was studied. The steel specimens irradiated by γ radiation for 3 months and 1 year were tested in saturated high-pressure bentonite (groundwater content 30%) for potential polarization curve. The fitting results were compared with that of the unirradiated specimens. **Figure 5** shows the corrosion current densities of steel unirradiated and irradiated for 3 months and 1 year in saturated highly compacted bentonite at different temperatures. The results found that the corrosion rate of irradiated steel is significantly higher than that without irradiation at high temperatures, and it increases with the irradiation time.

The maximum corrosion rate of steel irradiated for 3 months and 1 year occurred at the temperature of 348 K, corresponding to the 100 years in deep geological disposal. Because the voids of the compacted bentonite are initially filled with water, the oxygen concentration is low. Oxygen has not yet diffused on the metal surface. The maximum corrosion current density reaches 49.34 μA $cm^{-2}$ after 1 year of irradiation and reaches 17.24 μA $cm^{-2}$ after 3 months of irradiation, which was much higher than 0.77 μA $cm^{-2}$ without irradiation. With the increasing geological disposal year, the film of corrosion product is denser, and the temperature will continue to decrease. The content and diffusion of oxygen determine the cathodic reaction rate, so the corrosion current density of the specimen after radiation gradually decreases as the temperature decreases. However, it is still higher than that of unirradiated in the same period. The main reason is that γ irradiation changes the electrochemical state of metals, which is more obvious at higher temperatures. Liu et al. (2017) studied the corrosion behavior of X65 low-carbon steel unirradiated and irradiated in deep geological environments at

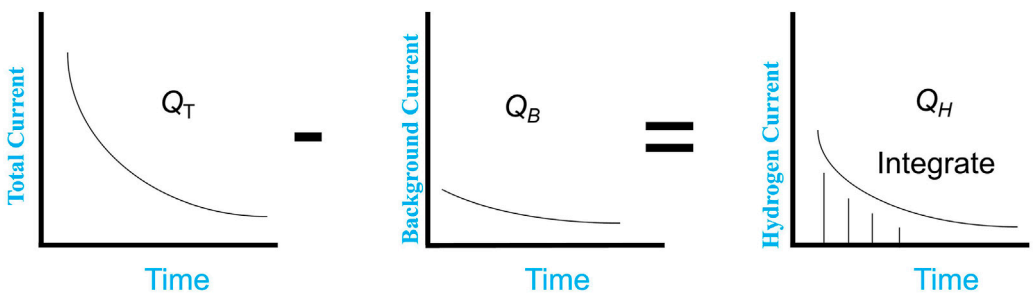


**FIGURE 4 |** Calculation method of hydrogen concentration.

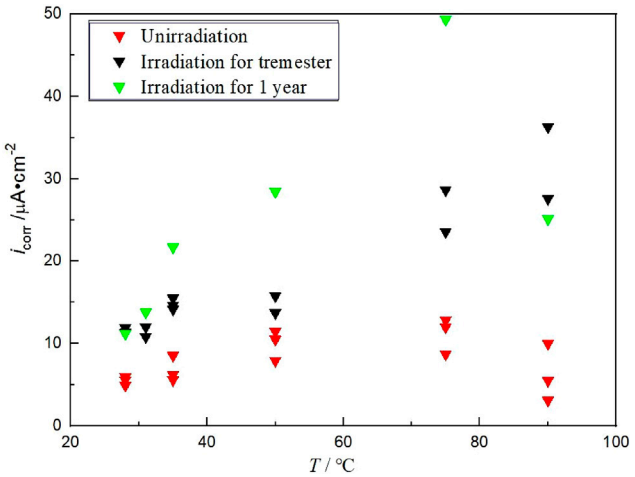


**FIGURE 5 |** Corrosion current density of Q235 steel unirradiated and irradiated for 3 months and 1 year in saturated highly compacted bentonite at different temperatures.

the temperature of 363 K. It was found that γ irradiation of 2.98 kGy h$^{-1}$ increased the corrosion rate of X65 steel by 33% and that γ irradiation caused two new phases of siderite and magnetite formed. Winsley et al. (2013) studied the effect of irradiation on the corrosion behavior of carbon steel in alkaline simulated pore water (pH = 13.4) at the temperature of 298 and 353 K. The corrosion rate is determined according to the hydrogen production. However, the results found that the hydrogen production rate did not increase significantly under γ radiation of 25 Gy h$^{-1}$. These results show that the effect of γ irradiation on the corrosion of carbon steel containers is obvious in a higher temperature environment.

The results discussed earlier indicate that γ irradiation could accelerate the corrosion of the steel at high temperatures. However, compared with the whole geological disposal period of nuclear waste containers, the high-temperature stage only exists for a short time. Meanwhile, it is predicted that after the disposal of HLNW, the initial irradiation dose rate on the outer surface of the HLNW container is approximately 0.2–2 Gy h$^{-1}$, then it will be reduced by one order of magnitude every 100 years according to the difference of vitrified solid waste, container, spatial layout, and thickness (Guo-ding, 2000; Dong et al., 2015). This shows that the radioactivity of nuclear waste will gradually weaken, and the effect of radiation on the container can be basically ignored in the large time-scale prediction. Therefore, the long-term corrosion rate model could refer to the prediction results of a previous study (Zhang et al., 2019).

## Hydrogen Permeation Efficiency of Carbon Steel During Corrosion in Highly-Pressed Saturated Bentonite

The results discussed earlier have shown that the effect of irradiation on the corrosion rate of carbon steel containers can be almost ignored on a large time scale. The hydrogen permeation behavior of carbon steel in a deep geological environment is studied based on the long-term corrosion rate model of carbon steel containers obtained in previous research (Zhang et al., 2019). Firstly, the hydrogen permeation law of carbon steel in a deep geological environment was explored. There are two main factors affecting the hydrogen permeation behavior of carbon steel containers in a deep geological environment, temperature and corrosion current density. The research was mainly carried out from these two influencing factors.

Because the buffer backfill material reaches saturation after 10 years, the saturation stage was focused on. The experimental medium is saturated, highly-compacted bentonite. Firstly, the hydrogen permeation law of steel in saturated highly compacted bentonite at different temperatures was studied. As shown in **Figure 6**, it is a variation of hydrogen concentration with time for steel in saturated highly pressed bentonite at different temperatures and different hydrogen charging current densities, in which a is 298 K, b is 313 K, c is 351 K, and d is 363 K (different temperatures correspond to a different year, as shown in **Figure 1**). The calculation method of hydrogen concentration has been introduced in *Experimental Method*. The results show that the hydrogen concentration increases in the steel with increasing hydrogen charging time at the same hydrogen charge current density. At the same hydrogen charging time, the hydrogen concentration in steel increases with the increase of the hydrogen charging current density; however, when the hydrogen charging current density increases to a certain extent, the increase of hydrogen concentration is no longer obvious. Each temperature has a similar pattern. This is because of the hydrogen evolution reaction on carbon steel. The generally accepted reaction scheme for proton reduction can be written as the Volmer reaction (Yan et al., 2007):

$$M + H^+ + e^- \rightarrow MH_{(ads)} \quad (2)$$

$$MH_{(ads)} + MH_{(ads)} \rightarrow 2M + H_2 \quad (3)$$

$$MH_{(ads)} \rightarrow MH_{(abs)} \quad (4)$$

Formula (2) refers to the adsorption of hydrogen, (3) refers to the recombination with hydrogen to form hydrogen molecules, and (4) refers to that some adsorbed H atoms may be absorbed into the lattice. When the hydrogen charging current density increases to a certain extent, reaction (2) is accelerated, resulting in the accumulation of a large amount of $MH_{(ads)}$ on the surface of carbon steel. Therefore, the adsorbed hydrogen binds faster, resulting in the escape of hydrogen. The results show that there is a linear law between the corrosion current density (the corrosion current density in the deep geological environment is much less than the experimental current density) and the hydrogen content in the carbon steel container at the same temperature, that is, the same disposal year.

**Figure 7** shows that the hydrogen concentration in steel changes with the charging time at different temperatures under the hydrogen charging current density of 10 A m$^{-2}$. At the same hydrogen charging current density and time, the hydrogen concentration in the steel increases with the rise in temperature. This shows that the hydrogen diffuses in the steel faster at high temperatures. The diffusion coefficient of hydrogen in steel is a function of temperature. Kiuchi and Mclellan (1986) comprehensively analyzed a large

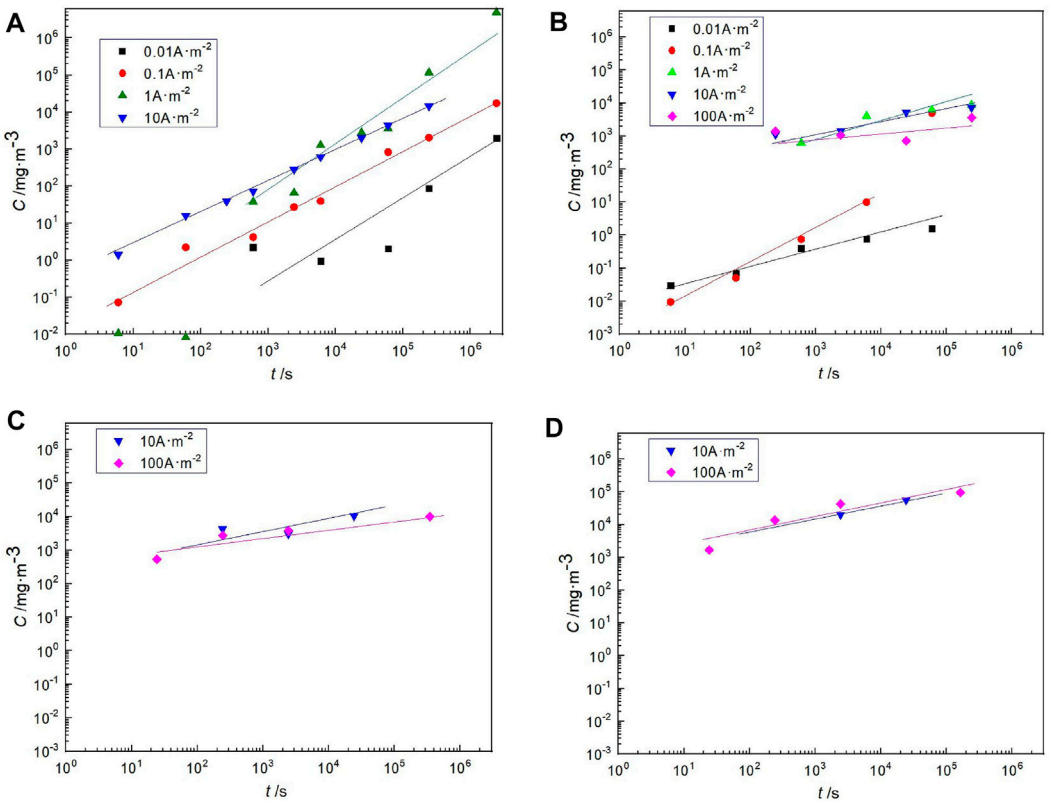


**FIGURE 6 |** Hydrogen concentration in Q235 steel with different current density of hydrogen charging in saturated highly compacted bentonite at different temperatures; **(A)** 298 K; **(B)** 313 K; **(C)** 351 K; **(D)**, 363 K.

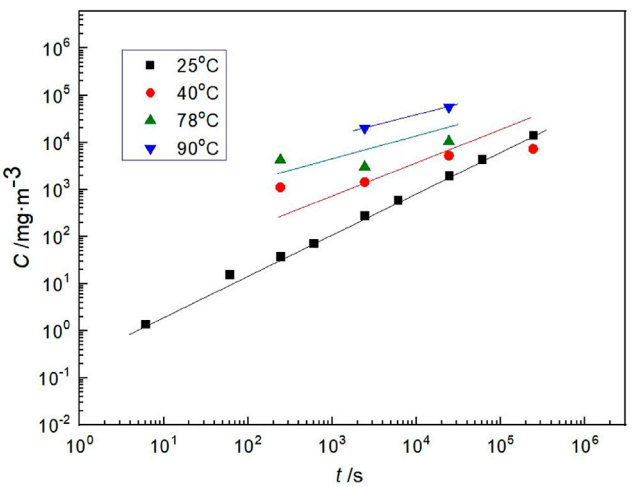


**FIGURE 7 |** Hydrogen concentration in Q235 steel with temperature at same charging current density of 10 A $m^{-2}$ in saturated highly compacted bentonite.

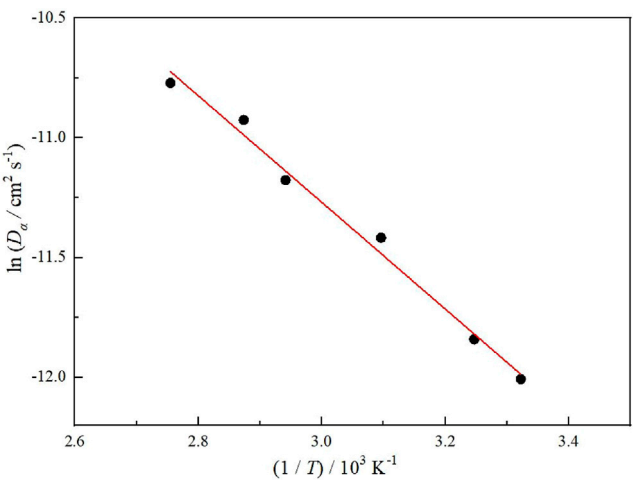


**FIGURE 8 |** Effect of temperature on hydrogen diffusivity of carbon steel in temperature range from 298 to 373 K

number of hydrogen diffusion data measured by various methods, indicating that the most representative equation of hydrogen diffusion coefficient is as follows:

$$D = 7.23 \times 10^{-8} \exp\left(-5.69\,(kJ/mol)/RT\right) m^2 s^{-1} \quad (5)$$

$$D = (1 \sim 2.52) \times 10^{-7} \exp\left[-(6.70 \sim 7.12)\,(kJ\,mol^{-1})/RT\right] m^2 s^{-1} \quad (6)$$

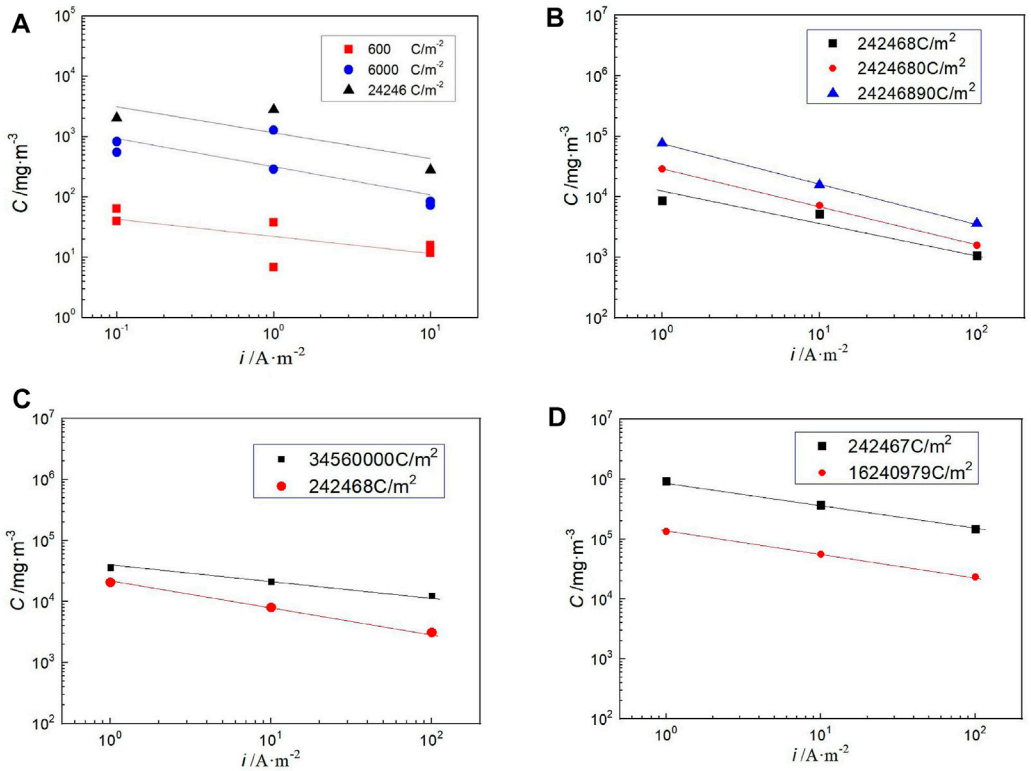


**FIGURE 9 |** Variation in hydrogen concentration in Q235 steel with charging current density for same fixed total charge at different temperatures in saturated highly compacted bentonite.

The temperature range is 233–353 K for **Equation 5** (323 to 823 K for **Equation 6**).

The diffusion coefficient of hydrogen in highly pressed saturated bentonite was also studied. The diffusivity can be calculated according to the following equation (Tsuru and Latanision, 1982):

$$t_b = 0.5\frac{L^2}{\pi^2 D_\alpha} \tag{7}$$

$D$ at different temperatures was counted by **Equation 7**. **Figure 8** gives the Arrhenius plot of hydrogen diffusivity $D$ against temperature.

$$D = 1.01 \times 10^{-6} \exp(-18.50\,(kJ/mol)/RT)\, m^2 s^{-1} \tag{8}$$

The fitted hydrogen diffusion coefficient equation is close to the research mentioned earlier (Kiuchi and Mclellan, 1986), which also shows that the deep geological environment has no effect on hydrogen diffusion in carbon steel.

The studies discussed earlier have obtained the relationship between temperature, current density, and hydrogen concentration in steel, but the total amount of hydrogen charging is different. **Figure 9** shows the relationship between the hydrogen concentration in steel and the hydrogen charging current density at different temperatures when the total amount of hydrogen charging is the same. The results show that the lower the hydrogen charging current density, the greater the hydrogen concentration in the steel for the same amount of hydrogen charging. This is also related to the hydrogen evolution reaction. Under the smaller hydrogen charging current density, the amount of adsorbed hydrogen produced in reaction (2) is relatively small, which is not enough to combine to generate the escaping hydrogen. So, more adsorbed hydrogen is transformed into absorbed hydrogen and enters the steel.

This study is to estimate the HPE on a large time scale. Obviously, hydrogen charging experiments for thousands of years cannot be completed in the laboratory. However, according to the relationship between hydrogen concentration, hydrogen charging current density, temperature, and the total amount of hydrogen charging in the research discussed earlier, as long as the amount of hydrogen charging in different disposal years could be obtained, the accelerated experiment could be completed in a short time using large hydrogen charging current density and finally predicted by extrapolation method. Previous studies have obtained the model of long-term corrosion rate for carbon steel in a deep geological environment, as shown in **Figure 10** (Zhang et al., 2019). The curve in **Figure 10** could be integrated to get the amount of hydrogen charging under natural corrosion conditions in different disposal years, as shown in **Table 4**.

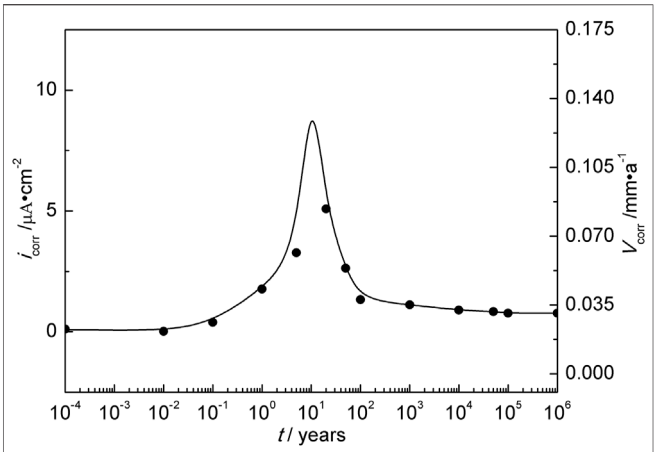


**FIGURE 10 |** Estimated corrosion rate of Q235 steel in deep geological disposal in Beishan area of China.

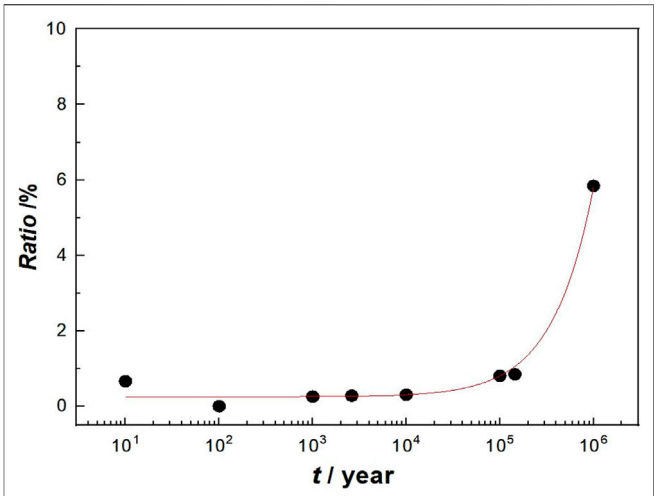


**FIGURE 12 |** Hydrogen permeation efficiency of Q235 steel in highly compacted bentonite at different disposal time.

**TABLE 4 |** Total amount of charge for hydrogen charging of carbon steel at different disposal periods under free corrosion conditions.

| *t*/year | 10 | 100 | 1,000 | 10,000 | 100,,000 |
|---|---|---|---|---|---|
| *Q* (C m$^{-2}$) | 1.6×10$^{7}$ | 1.1×10$^{8}$ | 4.6×10$^{8}$ | 3.0×10$^{9}$ | 2.6×10$^{10}$ |

Here, HPE is defined as the percentage of the hydrogen content in the steel to the total amount of hydrogen charging into the steel. Based on the linear relationship between hydrogen concentration and hydrogen charging current density (the total amount of hydrogen charging is the same), the HPE under natural corrosion conditions could be obtained by extrapolating the relationship curve between HPE and current density corresponding to hydrogen charging in different geological disposal years to the self-corrosion current density (**Figure 10**). As shown in **Figure 11A** is the result of 10 years, HPE is approximately 0.6%. 2) is the result of 100 years.

By analogy, it was acquired that the HPE of Q235 steel as HLNW container material in different deep geological disposal years, as shown in **Figure 12**. The results show that the HPE increases slowly with the disposal year. This result confirms the previously conjectured situation that the oxygen trapped after the container is buried is consumed through the corrosion reaction, which is related to the change from oxygen reduction to hydrogen reduction in the cathodic process of corrosion. Winsley et al. (2011) believe that when the oxygen content around the container drops to a low value, the hydrogen evolution reaction leads to the cathodic reaction. This result also implies that carbon steel containers are likely to suffer from HE in the medium and long term of deep geological disposal. The HE sensitivity of carbon steel containers in a deep geological environment is further judged by SSRT.

## Slow Strain Rate Tensile Test for Q235 Steel

The hydrogen diffusion in carbon steel is relatively fast, so HE sensitivity was studied by a control experiment. **Figure 13** shows the stress–strain curve for Q235 steel specimens; a is stretching in the air without any treatment, b is stretching in

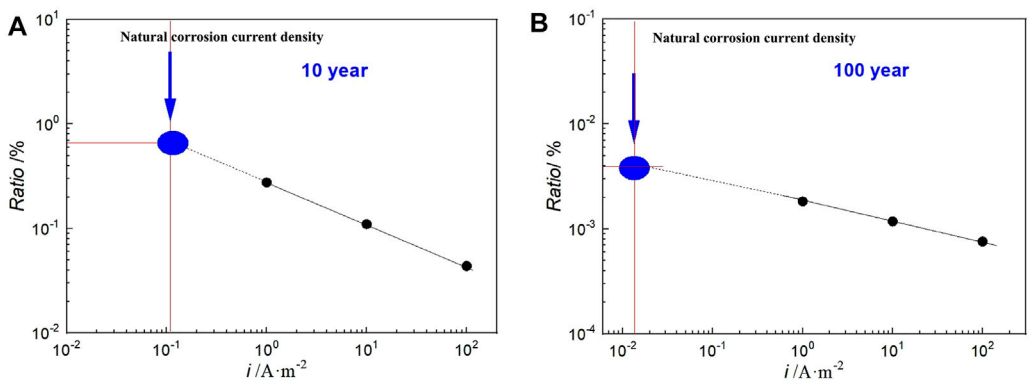


**FIGURE 11 |** Hydrogen permeation efficiency of Q235 steel in highly compacted bentonite with hydrogen charging density; **(A)** 10 years; **(B)** 100 years.

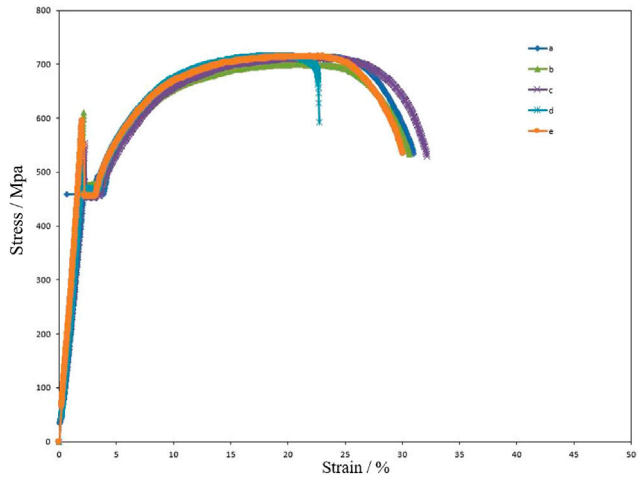


**FIGURE 13 |** Stress–strain curves for Q235 steel. **(A)** Original specimen; **(B)** specimen without treatment stretched in 0.2 mol $L^{-1}$ NaOH; **(C)** specimen stretched in air after hydrogen charged in 0.2 mol $L^{-1}$ NaOH solution for 7 days with 1 mA $cm^{-2}$; **(D)** specimen stretched in 0.2 mol $L^{-1}$ NaOH solution with 1 mA $cm^{-2}$ hydrogen charging and stretching at same time; **(E)** stretched in 0.2 mol $L^{-1}$L NaOH solution with 0.1 mA $cm^{-2}$ hydrogen charging and stretching at same time.

0.2 mol $L^{-1}$ NaOH solution without any treatment, c is stretching in the air after 7 days of hydrogen charging in 0.2 mol $L^{-1}$ NaOH solution, d is hydrogen charging under 1 mA $cm^{-2}$ and stretching in 0.2 mol $L^{-1}$ NaOH solution carried out at the same time, and e is hydrogen charging under 0.1 mA $cm^{-2}$ and stretching in 0.2 mol $L^{-1}$ NaOH solution carried out at the same time. The effect of tensile medium on tensile fracture elongation can be excluded by comparing a and b. **Figure 13C** shows that hydrogen cannot exist in Q235 steel for a long time and will escape quickly, so its fracture elongation is not affected. **Figure 13D** confirms that when hydrogen is always inside the steel, its fracture

**TABLE 5 |** Elongation of Q235 steel with different treatments and tensile methods (a, b, c, d, and e correspond to **Figure 5**).

| Curve | a | b | c | d | e |
|---|---|---|---|---|---|
| Elongation/% | 30.1 | 32.1 | 30.6 | 22.7 | 30.0 |

elongation decreases significantly. However, comparing d and e, it is found that when the hydrogen charging current density is too low, the hydrogen content in the steel is too low to reduce its fracture elongation. In short, Q235 steel is sensitive to HE when hydrogen is always present and when the content is high. **Table 5** summarizes the fracture elongation of specimens after different treatments.

**Figure 14** shows the morphology of the fracture surface for SSRT specimens. The original specimens a and b were stretched in air and 0.2 mol $L^{-1}$ NaOH solution, respectively; c is the hydrogen charging and stretching simultaneously in 0.2 mol $L^{-1}$ NaOH solution under 1 mA $cm^{-2}$. It can be seen obviously that a and b have dimple features, and large dimples are densely surrounded by small dimples, which represent the typical plastic fracture. After hydrogen charging under 1 mA $cm^{-2}$ in 0.2 mol $L^{-1}$ NaOH solution for 7 days, the specimen was stretched in the air. Also, the specimen was charged under 0.1 mA $cm^{-2}$ in 0.2 mol $L^{-1}$ NaOH solution and stretched. The fracture morphology of the two samples is similar to a and b. In **Figure 14C**, an obvious secondary crack can be seen. Furthermore, it is accompanied by a river pattern, which shows a brittle fracture. The result is consistent with **Figure 13**. For Q235 steel, only when its internal hydrogen content reaches a certain level and can exist for a long time will the material be sensitive to HE. Kobayashi et al. (2010) think that the amounts of hydrogen entering the elastic and the plastic deformation regions before the maximum stress had very little effect against the reduction of fracture strain. However, carbon steel container has been buried in a deep

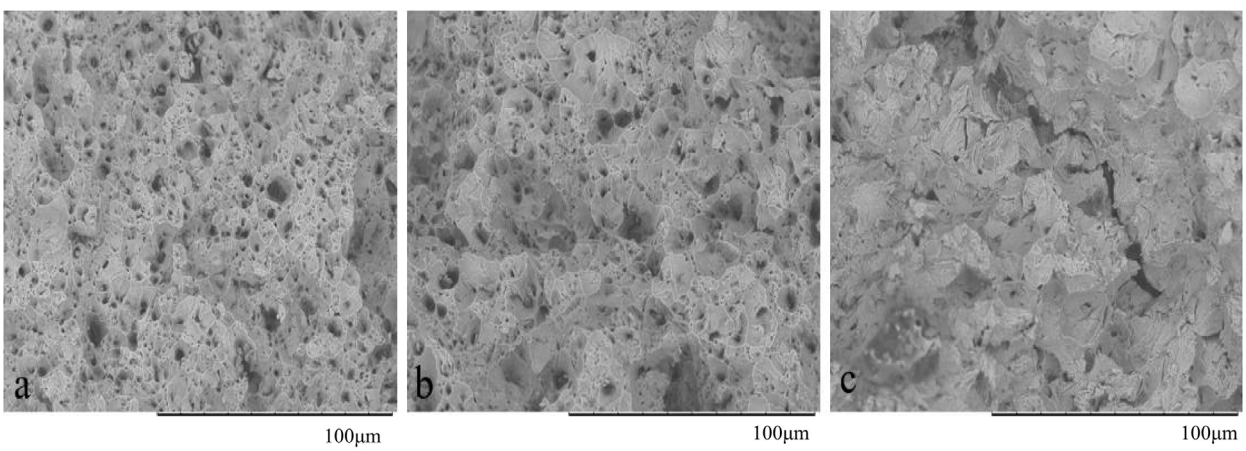


**FIGURE 14 |** Fracture morphologies of failed Q235 SSRT specimens; a and b are original specimens without treatment stretched in air and 0.2 mol $L^{-1}$ NaOH solution; c is specimen stretched in 0.2 mol $L^{-1}$ NaOH solution with 1 mA $cm^{-2}$ hydrogen charging and stretching at same time.

geological environment for tens of thousands or even hundreds of thousands of years. Due to the rapid diffusion of hydrogen in steel, it will continue to penetrate from the steel surface, and the corrosion current density (maximum corrosion current density is less than 10 μA $cm^{-2}$) is also far less than the hydrogen charging current density in the experiment. Hydrogen cannot exist in carbon steel for a long time and when the content is low. Although the HPE increases with the disposal year, the HE sensitivity of carbon steel containers is low. Thus, it is likely that the carbon steel container will not be damaged by HE.

## CONCLUSION

The HPE of Q235 steel as the nuclear waste container in a deep geological environment was predicted by the electrochemical method, and the possibility of hydrogen embrittlement was evaluated by a slow strain tensile test. The following conclusions are reached:

1) The radiation of nuclear waste will have a certain impact on the corrosion rate of the Q235 steel container, and the higher the temperature, the greater the corrosion rate. However, the high-temperature stage is very short, so it can be ignored that radiation's effect on the corrosion of container on a large time scale.
2) The longer the hydrogen permeation time, the higher the hydrogen concentration in the steel; under the same hydrogen charging time, the greater the hydrogen charging current, the greater the hydrogen concentration in the steel, but the hydrogen concentration does not increase when the current increases to a certain extent; under the same total hydrogen charging, the smaller the hydrogen charging current is, the greater the hydrogen concentration is.
3) The HPE during the corrosion process increases slowly with the increasing geological disposal age, which fully proves that the trapped oxygen is exhausted after the container is buried, and the cathodic process of corrosion changes from oxygen reduction to hydrogen reduction.
4) The Q235 steel will show hydrogen embrittlement sensitivity only when the internal hydrogen content reaches a certain level and can exist for a long time.

According to the conclusions discussed, although the HPE of Q235 steel increases, hydrogen will soon escape from the steel. So, it will show a low hydrogen embrittlement sensitivity from a large time scale for Q235 steel container. Therefore, Q235 steel as the nuclear waste container has a disadvantage of high corrosion rate and an advantage of low possibility of hydrogen embrittlement. Its thickness can be designed to be thicker to overcome the disadvantage.

## DATA AVAILABILITY STATEMENT

The original contributions presented in the study are included in the article/Supplementary Material, further inquiries can be directed to the corresponding authors.

## AUTHOR CONTRIBUTIONS

QZ has written the draft. YJ analyzed the data. XZ completed the part of the experiments. DL and YH provided guidance and funds. Other authors completed the revised manuscript, part of the experiments, and data.

## FUNDING

This work was financially supported by the National Natural Science Foundation of China under grant no. 51471160.

## REFERENCES

Arup, O. (1985). *Ocean Disposal of Radioactive Waste by Penetrator Emplacemen*. EUR 10170, London: Graham& Trotmon Let, For the Commission of European Communities.

Bradley, D. J. (1997). *Behind the Nuclear Curtain: Radioactive Waste-Management in the Former Soviet Union*. USA: UN Battelle Memorial Institute.

Dong, L., Zhongtian, Y., Weibing, Y., Qinghong, S., and Wei, L. (2015). Preliminary Study on Gamma Radiation Effects on Modified Sodium Bentonite[J]. *Acta Mineralogica Sinica* 35 (1), 103–106.

Duquette, D. J., Latanision, R. M., Di Bella, C. A. W., and Kirstein, B. E. (2009). Corrosion Issues Related to Disposal of High-Level Nuclear Waste in the Yucca Mountain Repository-Peer Reviewers' Perspective. *Corrosion* 65, 272–280. doi:10.5006/1.3319133

Ewing, R. C. (2015). Long-term Storage of Spent Nuclear Fuel. *Nat. Mater* 14, 252–257. doi:10.1038/nmat4226

Guo, X., Gin, S., Lei, P., Yao, T., Liu, H., Schreiber, D. K., et al. (2020). Self-accelerated Corrosion of Nuclear Waste Forms at Material Interfaces. *Nat. Mater.* 19, 310–316. doi:10.1038/s41563-019-0579-x

Guo-ding, L. I. (2000). Coupled Calculation of Dose Rate and Temperature in the Near Field of a High-Level Radioactive Waste Disposal Repository[J]. *Radiat. Prot.* 20 (3), 153–158. doi:10.1093/rpd/ncx054

Hu, Y., and Cheng, H. (2015). Disposal Capacity for Spent Fuel in China Is Not Ready yet for the Nuclear Power Boom. *Environ. Sci. Technol.* 49, 2596–2597. doi:10.1021/es505855s

Huang, Y., and Zhu, Y. (2005). Hydrogen Ion Reduction in the Process of Iron Rusting. *Corrosion Sci.* 47 (6), 1545–1554. doi:10.1016/j.corsci.2004.07.044

King, F., and Padovani, C. (2011). Review of the Corrosion Performance of Selected Canister Materials for Disposal of UK HLW And/or Spent Fuel. *Corrosion Eng. Sci. Tech.* 46, 82–90. doi:10.1179/1743278211y.0000000005

Kiuchi, K., and Mclellan, R. B. (1986). The Solubility and Diffusivity of Hydrogen in Well-Annealed and Deformed Iron. *Acta Metallurgica* 31, 29–52. doi:10.1016/b978-0-08-034813-1.50009-7

Kobayashi, M., Nishikata, A., and Tsuru, T. (2010). Effect of Stain Rate and Hydrogen Charging Current on Hydrogen Embrittlement of Carbon Steel in High Alkaline Chloride Environment. *Zakaep* 59 (4), 129–135. doi:10.3323/jcorr.59.129

Liu, C., Tian, C., Zhang, Z., Han, E. H., and Wang, J. (2019). Corrosion Behaivour of X65 Low Carbon Steel during Anaerobic Period of High Level Nuclear Waste Disposal. *Corrosion Sci. Prot. Tech.* 31, 371–378. doi:10.11900/0412.1961.2018.00481

Liu, C., Tian, C., Zhang, Z., Han, E. H., and Wang, J. (2019). Corrosion Behaivour of X65 Low Carbon Steel during Redox State Transition Process of High Level Nuclear Waste Disposal. *Acta Metallurgica Sinica* 55, 849–858. doi:10.11900/0412.1961.2018.00481

Liu, C., Wang, J., Zhang, Z., Han, E.-H., Liu, W., Liang, D., et al. (2018). Effect of Cumulative Gamma Irradiation on Microstructure and Corrosion Behaviour of X65 Low Carbon Steel. *J. Mater. Sci. Tech.* 34, 2131–2139. doi:10.1016/j.jmst.2018.03.017

Liu, C., Wang, J., Zhang, Z., and Han, E.-H. (2017). Studies on Corrosion Behaviour of Low Carbon Steel Canister with and without γ-irradiation in China's HLW Disposal Repository. *Corrosion Eng. Sci. Tech.* 52 (Suppl. 1), 136–140. doi:10.1080/1478422x.2017.1348762

Milnes, A. G. (1985). *Geology and Radwaste*. New York: Academic Press.

Rasilainen, K. (2004). *Localisation of the SR 97 Process Report for Posiva's Spent Fuel Repository at Olkiluoto[R]*. Finland: Department of Mathematics and Systems Analysis.

Rosborg, B., and Werme, L. (2008). The Swedish Nuclear Waste Program and the Long-Term Corrosion Behaviour of Copper[J]. *J. Nucl. Mater.* 379 (1-3), 142–153. doi:10.1016/j.jnucmat.2008.06.025

Seetharam, S. C., Cleall, P. J., and Thomas, H. R. (2006). Modelling Some Aspects of Ion Migration in a Compacted Bentonitic Clay[J]. *Eng. Geology.* 85 (1-2), 221–228. doi:10.1016/j.enggeo.2005.09.041

Shoesmith, D. W. (2000). Fuel Corrosion Processes under Waste Disposal Conditions. *J. Nucl. Mater.* 282, 1–31. doi:10.1016/s0022-3115(00)00392-5

Smart, N. R., Rance, A. P., and Werme, L. O. (2008). The Effect of Radiation on the Anaerobic Corrosion of Steel. *J. Nucl. Mater.* 379, 97–104. doi:10.1016/j.jnucmat.2008.06.007

Stoulil, J., Kaňok, J., Kouřil, M., Parschová, H., and Novák, P. (2013). Influence of Temperature on Corrosion Rate and Porosity of Corrosion Products of Carbon Steel in Anoxic Bentonite Environment. *J. Nucl. Mater.* 443, 20–25. doi:10.1016/j.jnucmat.2013.06.031

Tsuru, T., Huang, Y., Ali, M. R., and Nishikata, A. (2005). Hydrogen Entry into Steel during Atmospheric Corrosion Process. *Corrosion Sci.* 47 (10), 2431–2440. doi:10.1016/j.corsci.2004.10.006

Tsuru, T., and Latanision, R. M. (1982). Grain Boundary Transport of Hydrogen in Nickel. *Scripta Metallurgica* 16, 575–578. doi:10.1016/0036-9748(82)90273-3

Winsley, R. J., Smart, N. R., Rance, A. P., Fennell, P. A. H., Reddy, B., and Kursten, B. (2011). Further Studies on the Effect of Irradiation on the Corrosion of Carbon Steel in Alkaline media. *Corrosion Eng. Sci. Tech.* 46 (2), 111–116. doi:10.1179/1743278210y.0000000010

Winsley, R. J., Smart, N. R., Rance, A. P., Fennell, P. A. H., Reddy, B., and Kursten, B. (2013). Further Studies on the Effect of Irradiation on the Corrosion of Carbon Steel in Alkaline media. *Corrosion Eng. Sci. Tech.* 46 (2), 111–116. doi:10.1179/1743278210y.0000000010

Yan, L., Ramamurthy, S., Noel, J. J., and Shoesmith, D. W. (2007). Hydrogen Absorption into Alpha Titanium in Acidic Solutions. *Electrochim. Acta* 52, 1169e1181. 10.1016/j.electacta.2006.07.017.

Yang, C., Samper, J., and Montenegro, L. (2008). A Coupled Non-isothermal Reactive Transport Model for Long-Term Geochemical Evolution of a HLW Repository in clay. *Environ. Geol.* 53 (8), 1627–1638. doi:10.1007/s00254-007-0770-2

Zhang, L., Zhao, W., Li, Y., and Li, S. (2013). Probabilistic Assessment of Failure for Low-Medium Level Nuclear Waste Storage Container. *Chin. J. Appl. Mech.* 30 (2), 287–290. 10.11776/cjam.30.02.D015.

Zhang, Q., Huang, Y., Blackwood, D. J., Zhang, B., Lu, D., Yang, D., et al. (2020). On the Long Term Estimation of Hydrogen Embrittlement Risks of Titanium for the Fabrication of Nuclear Waste Container in Bentonite Buffer of Nuclear Waste Repository. *J. Nucl. Mater.* 533, 152092. doi:10.1016/j.jnucmat.2020.152092

Zhang, Q., Zheng, M., Huang, Y., Kunte, H. J., Wang, X., Liu, Y., et al. (2019). Long Term Corrosion Estimation of Carbon Steel, Titanium and its alloy in Backfill Material of Compacted Bentonite for Nuclear Waste Repository. *Sci. Rep.* 9, 3195. doi:10.1038/s41598-019-39751-9

Zheng, M., Zhang, Q., Huang, Y., Lu, D., Yu, X., Liu, Y., et al. (2016). Determination of Representative Ground-Water for Corrosion Assessment of Candidate Materials Used in Beishan Area Preselected for High-Level Radioactive Waste Disposal Repository[J]. *J. Chin. Soc. Corrosion Prot.* 36 (2), 185–190. doi:10.11902/1005.4537.2015.055

**Conflict of Interest:** The authors declare that the research was conducted in the absence of any commercial or financial relationships that could be construed as a potential conflict of interest.

**Publisher's Note:** All claims expressed in this article are solely those of the authors and do not necessarily represent those of their affiliated organizations or those of the publisher, the editors, and the reviewers. Any product that may be evaluated in this article, or claim that may be made by its manufacturer, is not guaranteed or endorsed by the publisher.